



HAL
open science

Global-Local non intrusive analysis with robin parameters: application to plastic hardening behavior and crack propagation in 2D and 3D structures

Ignacio Fuenzalida-Henriquez, Paul Oumaziz, Emilio Castillo-Ibarra, Jorge Hinojosa

► **To cite this version:**

Ignacio Fuenzalida-Henriquez, Paul Oumaziz, Emilio Castillo-Ibarra, Jorge Hinojosa. Global-Local non intrusive analysis with robin parameters: application to plastic hardening behavior and crack propagation in 2D and 3D structures. Computational Mechanics, In press, 10.1007/s00466-021-02124-z. hal-03613766

HAL Id: hal-03613766

<https://hal.science/hal-03613766>

Submitted on 18 Mar 2022

HAL is a multi-disciplinary open access archive for the deposit and dissemination of scientific research documents, whether they are published or not. The documents may come from teaching and research institutions in France or abroad, or from public or private research centers.

L'archive ouverte pluridisciplinaire **HAL**, est destinée au dépôt et à la diffusion de documents scientifiques de niveau recherche, publiés ou non, émanant des établissements d'enseignement et de recherche français ou étrangers, des laboratoires publics ou privés.

Global-Local Non Intrusive Analysis with Robin Parameters: Application to Plastic Hardening behavior and Crack Propagation in 2D and 3D Structures

Ignacio Fuenzalida-Henriquez¹ Paul Oumaziz² Emilio Castillo-Ibarra³
Jorge Hinojosa⁴

¹ Building Management and Engineering Department, Universidad de Talca, Curicó, Chile Engineering Systems Doctoral Program, Universidad de Talca, Curicó, Chile E-mail: ifuenzalida@utalca.cl

² Institut Clément Ader, Université de Toulouse, CNRS UMR5312, INSA/ISAE-SUPAERO/IMT Mines Albi/UPS, Toulouse, France

E-mail: paul.oumaziz@insa-toulouse.fr ³ Engineering Systems Doctoral Program, Universidad de Talca, Curicó, Chile E-mail: emcastillo@utalca.cl

⁴ Industrial Technologies Department, Universidad de Talca, Curicó, Chile E-mail: jhinojosa@utalca.cl

Abstract

The global/local analysis allows to embed a specific local zone of interest with a different behaviour in a global coarse model. In this local model, fine meshes are usually used to model some structural details and potentially non-linear behaviours, such as plastic hardening and crack propagation. The standard global/local approach can be observed as a Dirichlet-Neumann iterative algorithm where a Dirichlet problem on the local model and a Neumann problem on the global one are solved successively. This paper proposes a new approach for the global/local framework as Robin parameters are considered on both local and global models to obtain more flexibility and improvement for convergence. Particularly, Robin parameters are obtained using a pre-defined strip of elements and the results are later improved by means of single-objective optimization, minimizing the number of iterations to achieve convergence. This improvement is illustrated for cracked domains and plastic hardening in 2D problems and 3D elements within a non-intrusive framework, allowing the usage of commercial finite element software along with open-source research finite element software.

Keywords: Global Local Robin Parameter Crack Propagation Patch Hardening

1 Introduction

The objective of non-intrusive frameworks is to carry out advanced numerical methods as a result of efficient linear and non-linear solvers applied in the commercial software and used as “black boxes”. An example of the above is that it is feasible to operate the free open-source industrial finite elements software *code-aster* [12] with the *Python* interface. Advanced algorithms can be designed within this *Python* interface and call non-linear methods of *code-aster* to consider complex phenomena. In addition, depending on the perspective, the non-intrusivity might be the alternative to “enrich” a global model with those that are more detailed and without modifying the global one. For example, the global model could be the product of a long industrial process, which might not be altered easily. In this regard, methods considering local models without altering the global one can be perceived as non-intrusive.

The global/local approach [38] is a very good option for implementing the non-intrusive method [16]. In essence, the idea is to introduce some more localized details into a global and coarse model and potentially add non-linear behaviours in specific areas without altering the global model. Summarizing, a global and a local model connected

This paper is an extended version of our paper published in 14th World Congress on Computational Mechanics (WCCM). doi:10.23967/wccm-eccomas.2020.159

through an interface coexist. The global/local approach is about an iterative Dirichlet-Neumann algorithm and an iteration consisting of two steps: (1) a problem in the local model with Dirichlet boundary conditions on the interface, and (2) a problem in the global model with Neumann boundary conditions on the interface. Connections with optimized Schwarz domain decomposition methods can be observed in [18]. The global/local structure has been expanded to a domain decomposition method [11] and has been implemented to different types of non-linearities such as crack propagation [32, 11, 28], structural joints and assemblies [19], local plasticity [16] and cycling visco-elastic behaviour [4]. It is possible to find other studies regarding different applications and improvements for non-intrusive frameworks and the global/local method in [23, 15, 17, 18, 6, 1].

Considering the St. Venant’s principle, the interface between the local and global models should be nowhere near the local details to avoid the inaccuracy of the Dirichlet boundary conditions from the linear global model close to the area of potential non-linearity. This problem could be solved by using Robin parameters on the interface. The first proposal to apply Robin parameters on the interface for a local plastic model can be found in [15]. Their idea is to design a ”quasi-optimal” Robin parameter avoiding the full computation of the Schur complement of the complementary models. They prefer two-scale Robin parameters that include both short and long-range effects. Very recent works [28, 1] applied a global/local approach with Robin conditions for phase field modelling for mechanical and hydraulic fractures in porous media. They chose the Schur complement of the complementary domain and observed very good performance, improving drastically the convergence of the global/local algorithm.

Finally, a formal mathematical approach to Mixed Domain Decomposition Methods and the application for non-intrusive analysis with Robin Parameters can be found in [27, 31, 28].

This paper focuses on the global/local method with a non-intrusive implementation of Robin parameters on the interface. These Robin parameters are developed with a strip of elements linked to the interface similarly as [15]. The choice of these Robin parameters is crucial for the convergence of the method. The optimal choice is classically known but with an unaffordable cost as it would involve the computation of a Schur complement of a large model. Therefore, approximations are sought and we propose to carry out an optimization of the parameters to obtain a better convergence of the mixed method for the global/local analysis and study the impact of the Robin parameter as well.

The article is structured as follows: Section 2 formulates the global/local method as a Dirichlet-Neumann algorithm; Section 3 pursues the global/local method with the Robin parameters; Section 4 and subsequent sections illustrate the improvements of our implementation with numerical examples and different non-linear problems in 2D and 3D models, as well as the optimization of the Robin parameters.

2 Global/Local Problem Formulation

2.1 Reference problem

A mechanical model of a structure determined on a domain Ω_R is considered. This domain consists of two non-overlapping domains Ω_C , the complementary domain, and Ω_L , the local domain. Ω_C considers elastic linear isotropic assumptions with small perturbations, meanwhile in Ω_L , the mechanical model may be non-linear, such as a crack propagation model or a plastic material. This local model allows embedding localized richer contents in the structure’s simple global model. Γ is noted as the interface between the complementary and local models.

Defining the admissible space of displacements as:

$$V(\Omega_R) = \{v \in H_1(\Omega_R) \mid v = u_d \text{ on } \partial_u \Omega_R\} \quad (1)$$

The mechanical problem is equivalent to:

$$\text{Find } u \in V(\Omega_R), \quad a_R(u, v) = l_R(v), \quad \forall v \in V_0(\Omega_R) \quad (2)$$

with a_R the bi-linear form representing the structure’s equilibrium and l_R the linear form symbolizing the Neumann boundary conditions. The Dirichlet boundary conditions are taken into account in the affine space $V(\Omega_R)$.

A discretization of standard finite elements with Lagrange shape functions is considered in order to obtain discrete models for which a conforming mesh in the interface between the complementary and local models is adopted.

A full elastic linear isotropic material over the whole domain $\Omega_R = \Omega_C \cup \Omega_L$ is considered to detail the methods and the equation. Under this type of hypothesis, the discrete problem becomes as follows:

$$\text{Find } \mathbf{u}_R \text{ solution of } \mathbf{K}_R \mathbf{u}_R = \mathbf{f}_d^R \quad (3)$$

with \mathbf{K}_R the stiffness matrix, \mathbf{u}_R the discrete unknown of displacements and \mathbf{f}_d^R the right-hand side conforming to the boundary conditions. The null Dirichlet conditions are expected to be eliminated.

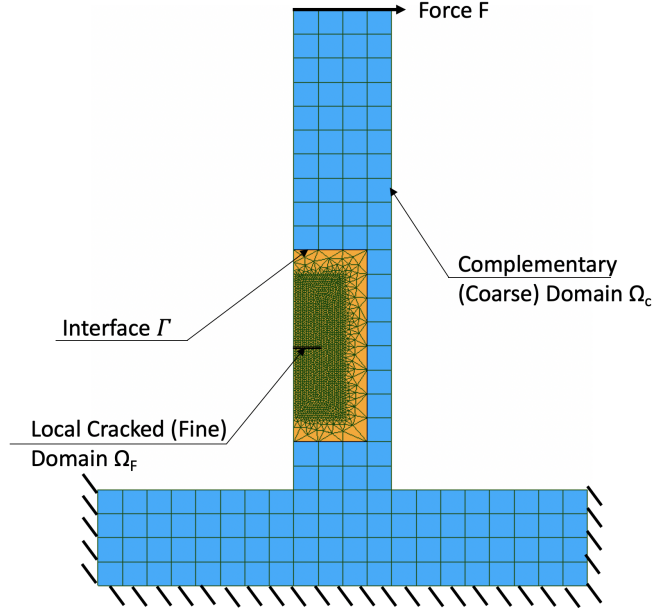


Figure 1: Reference problem.

This reference problem can be seen as the coupling between the complementary model in Ω_C and the local model in Ω_L , as presented in Figure 1. We note that \mathbf{K}_C and \mathbf{K}_L are the stiffness matrices of the complementary and local models respectively, \mathbf{u}_C and \mathbf{u}_L are the displacements in Ω_C and Ω_L , \mathbf{f}_d^C and \mathbf{f}_d^L are the load vectors in Ω_C and Ω_L . The perfect coupling of the two models to impose the continuity of the displacement is enforced with a Lagrange multiplier $\boldsymbol{\lambda}$ into the following Lagrangian:

$$\mathcal{L}(\mathbf{u}_C, \mathbf{u}_L, \boldsymbol{\lambda}) = \frac{1}{2} \mathbf{u}_C^T \mathbf{K}_C \mathbf{u}_C + \frac{1}{2} \mathbf{u}_L^T \mathbf{K}_L \mathbf{u}_L - \mathbf{f}_d^{C^T} \mathbf{u}_C - \mathbf{f}_d^{L^T} \mathbf{u}_L + \boldsymbol{\lambda}^T (\mathbf{C}_C \mathbf{u}_C - \mathbf{C}_L \mathbf{u}_L) \quad (4)$$

Where \mathbf{C}_C and \mathbf{C}_L are coupling operators. For conforming meshes, these are trace operators that extract displacements from Ω_C and Ω_L on the interface Γ . They are sparse matrices filled with number ones in the indexes associated to the interface degrees of freedom.

The minimization of the Lagrangian leads to:

- Equilibrium of the coarse model:

$$\frac{\partial \mathcal{L}}{\partial \mathbf{u}_C} = \mathbf{K}_C \mathbf{u}_C + \mathbf{C}_C^T \boldsymbol{\lambda} - \mathbf{f}_d^C = 0 \quad (5)$$

- Equilibrium of the local model:

$$\frac{\partial \mathcal{L}}{\partial \mathbf{u}_L} = \mathbf{K}_L \mathbf{u}_L - \mathbf{C}_L^T \boldsymbol{\lambda} - \mathbf{f}_d^L = 0 \quad (6)$$

- Continuity of the interface displacements:

$$\mathbf{C}_C \mathbf{u}_C - \mathbf{C}_L \mathbf{u}_L = 0 \quad (7)$$

70 Therefore we obtain the standard coupling system:

$$\text{Find } (\mathbf{u}_C, \mathbf{u}_L, \boldsymbol{\lambda}), \quad \begin{bmatrix} \mathbf{K}_C & 0 & -\mathbf{C}_C^T \\ 0 & \mathbf{K}_L & \mathbf{C}_L^T \\ -\mathbf{C}_C & \mathbf{C}_L & 0 \end{bmatrix} \begin{bmatrix} \mathbf{u}_C \\ \mathbf{u}_L \\ \boldsymbol{\lambda} \end{bmatrix} = \begin{bmatrix} \mathbf{f}_d^C \\ \mathbf{f}_d^L \\ 0 \end{bmatrix} \quad (8)$$

This problem can be rewritten as two sub-problems: one over Ω_C with Neumann conditions of the interface Γ and the other problem over Ω_L with Dirichlet conditions on the interface Γ :

$$\begin{aligned} \text{Find } \mathbf{u}_C, \quad \mathbf{K}_C \mathbf{u}_C &= \mathbf{f}_d^C + \mathbf{C}_C^T \boldsymbol{\lambda} \\ \text{Find } (\mathbf{u}_L, \boldsymbol{\lambda}), \quad \begin{bmatrix} \mathbf{K}_L & \mathbf{C}_L^T \\ \mathbf{C}_L & 0 \end{bmatrix} \begin{bmatrix} \mathbf{u}_L \\ \boldsymbol{\lambda} \end{bmatrix} &= \begin{bmatrix} \mathbf{f}_d^L \\ -\mathbf{C}_C \mathbf{u}_C \end{bmatrix} \end{aligned} \quad (9)$$

A Dirichlet-Neumann iterative algorithm is used to solve this problem. The iteration consists in the following two steps:

1. Knowing a $(\mathbf{u}_L^n, \boldsymbol{\lambda}^n)$ solution in Ω_L to solve a Neumann problem on Ω_C :

$$\text{Find } \mathbf{u}_C^{n+1}, \quad \mathbf{K}_C \mathbf{u}_C^{n+1} = \mathbf{f}_d^C + \mathbf{C}_C^T \boldsymbol{\lambda}^n \quad (10)$$

2. Knowing a \mathbf{u}_C^{n+1} solution in Ω_C to solve a Dirichlet problem on Ω_L :

$$\text{Find } (\mathbf{u}_L^{n+1}, \boldsymbol{\lambda}^{n+1}), \quad \begin{bmatrix} \mathbf{K}_L & \mathbf{C}_L^T \\ \mathbf{C}_L & 0 \end{bmatrix} \begin{bmatrix} \mathbf{u}_L^{n+1} \\ \boldsymbol{\lambda}^{n+1} \end{bmatrix} = \begin{bmatrix} \mathbf{f}_d^L \\ \mathbf{C}_C \mathbf{u}_C^{n+1} \end{bmatrix} \quad (11)$$

75 and obtain $\boldsymbol{\lambda}^{n+1}$, the opposite of the reaction forces $\boldsymbol{\lambda}_L^{n+1}$ on the interface of the local model.

Remark 1. *This type of algorithm could be considered with multiple local models and conceived as a non-overlapping domain decomposition [11].*

2.2 Primal-Dual Global/Local Analysis

80 The subtlety of the global/local method is to slightly modify the problem in the complementary domain with the aim of not solving it in Ω_C , but in a “global” domain Ω_G , which corresponds to the union of Ω_C and an auxiliary domain Ω_A . Globally, this auxiliary domain corresponds geometrically to the local domain Ω_L but coarsely meshed as the complementary model. As shown in Figure 2, the local model is substituted by an auxiliary model to obtain a global model.

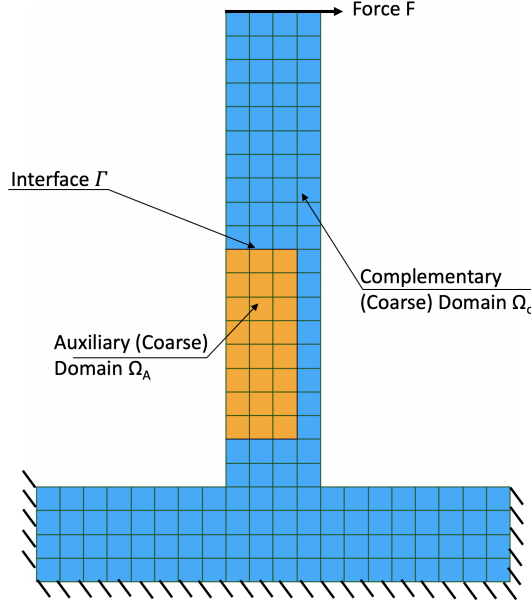


Figure 2: Linear problem.

This can also be interpreted differently. Starting from a global model with a coarse mesh and an elastic linear isotropic material, this model can be enriched with localized details such as structural details (holes or a particular geometry) or complex non-linear behaviour (plasticity or cracks). This is especially suitable in an industrial design process where the global model may not be easily changed to incorporate localized details.

The complementary problem to be solved is defined as:

$$\text{Find } \mathbf{u}_C^{n+1}, \mathbf{K}_C \mathbf{u}_C^{n+1} = \mathbf{f}_d^C + \mathbf{C}_C^T \boldsymbol{\lambda}^n \quad (12)$$

The contribution of the auxiliary model is added to the two sides of the equation where the exponent $n + 1$ and n are omitted in order to simplify the notations:

$$\overline{\mathbf{K}}_C \overline{\mathbf{u}}_C + \overline{\mathbf{K}}_A \overline{\mathbf{u}}_A = \underbrace{\overline{\mathbf{f}}_d^C + \overline{\mathbf{f}}_d^A}_{\mathbf{f}_d^G} + \mathbf{C}_G^T \boldsymbol{\lambda} + \underbrace{\overline{\mathbf{K}}_A \overline{\mathbf{u}}_A - \overline{\mathbf{f}}_d^A}_{\mathbf{C}_G^T \boldsymbol{\lambda}_A} \quad (13)$$

where the notation $\overline{\square}_X$ means that the variable or operator \square specified in Ω_X is extended with zeros to the domain Ω_C for the rest of the degrees of freedom. In addition, $\overline{\mathbf{f}}_d^A$ corresponds to the boundary conditions that could be implemented on the auxiliary model in order to represent an approximation of those on the local model. The term $\overline{\mathbf{K}}_A \overline{\mathbf{u}}_A - \overline{\mathbf{f}}_d^A$ symbolizes the reaction forces of a Dirichlet problem on the auxiliary model with displacement $\mathbf{u}_{G|\Gamma}$ imposed in Γ and a Neumann boundary condition through $\overline{\mathbf{f}}_d^A$. For more details see [18].

Therefore, as $\overline{\mathbf{u}}_C = \overline{\mathbf{u}}_A$ on the interface Γ , the equation becomes as follows:

$$\begin{aligned} \mathbf{K}_G \mathbf{u}_G^{n+1} &= \mathbf{f}_d^G + \mathbf{C}_G^T \boldsymbol{\lambda}^n + \mathbf{C}_G^T \boldsymbol{\lambda}_A^n \\ &= \mathbf{f}_d^G + \mathbf{C}_G^T \mathbf{P}^n \end{aligned} \quad (14)$$

with \mathbf{u}_G^{n+1} the displacement specified on the global model. The reaction forces $\boldsymbol{\lambda}_A^n$ are computed with displacement \mathbf{u}_G^n from the previous iteration of the algorithm. $\mathbf{P}^n = \boldsymbol{\lambda}_A^n - \boldsymbol{\lambda}_L^n$ represents the correction of forces that will be applied to the global model in order to consider the local model. It can also be observed that \mathbf{P}^n verifies the following equations assuming exact solutions for the global and local problems [18]:

$$\begin{aligned} \mathbf{P}^n &= \boldsymbol{\lambda}_A^{n+1} + \boldsymbol{\lambda}_C^{n+1} \\ \mathbf{P}^{n+1} &= \mathbf{P}^n + \mathbf{r}^{n+1} \text{ with } \mathbf{r}^{n+1} = -(\boldsymbol{\lambda}_L^{n+1} + \boldsymbol{\lambda}_C^{n+1}) \end{aligned} \quad (15)$$

Under this notation, \mathbf{r}^{n+1} represents the disequilibrium of forces between the complementary model and the local model. When convergence is fulfilled, $\mathbf{r}^{n+1} = 0$ and the forces are balanced: the solution on $\Omega_C \cap \Omega_L$ reaches the solution of the reference model.

The error indicator for the convergence of the method is the residual norm for each iteration normalized regarding the first residual obtained from global/local iterations, as presented in Eq. (16).

$$\eta = \frac{\|\mathbf{r}^{n+1}\|_2}{\|\mathbf{r}^0\|_2} \quad (16)$$

2.3 Global/Local algorithm

The iterations described above lead to the algorithm 1 of the global/local method.

Algorithm 1 Global/Local Primal-Dual Solution

1: Initialize interface vector $\mathbf{P}^0 = 0$

2: Initialize error $\eta = 1$ and tolerance tol

3: Start iterations, $n = 0$

4: **while** $\eta > tol$ **do**

5: Solve the global problem:

$$\text{Find } \mathbf{u}_G^{n+1}, \mathbf{K}_G \mathbf{u}_G^{n+1} = \mathbf{f}_d^G + \mathbf{C}_G^T \mathbf{P}^n$$

6: Solve the auxiliary problem to compute λ_A^{n+1} :

$$\text{Find } (\mathbf{u}_A, \lambda_A^{n+1}), \begin{bmatrix} \mathbf{K}_A & \mathbf{C}_A^T \\ \mathbf{C}_A & 0 \end{bmatrix} \begin{bmatrix} \mathbf{u}_A \\ -\lambda_A^{n+1} \end{bmatrix} = \begin{bmatrix} \mathbf{f}_d^A \\ \mathbf{C}_G \mathbf{u}_G^{n+1} \end{bmatrix}$$

7: Solve the local problem:

$$\text{Find } (\mathbf{u}_L^{n+1}, \lambda^{n+1}), \begin{bmatrix} \mathbf{K}_L & \mathbf{C}_L^T \\ \mathbf{C}_L & 0 \end{bmatrix} \begin{bmatrix} \mathbf{u}_L^{n+1} \\ \lambda^{n+1} \end{bmatrix} = \begin{bmatrix} \mathbf{f}_d^L \\ \mathbf{C}_G \mathbf{u}_G^{n+1} \end{bmatrix}$$

8: Compute the new \mathbf{P}^{n+1} :

$$\mathbf{P}^{n+1} = \lambda_A^{n+1} + \lambda^{n+1}$$

9: Calculate the residual of the iteration $\mathbf{r}^{n+1} = \mathbf{P}^{n+1} - \mathbf{P}^n$

10: Update the new \mathbf{P}^{n+1} including relaxation factor μ :

$$\mathbf{P}^{n+1} = \mu \mathbf{P}^{n+1} + (1 - \mu) \mathbf{P}^n$$

11: Estimate the error of the iteration step as $\eta = \|\mathbf{r}^{n+1}\|_2 / \|\mathbf{r}^0\|_2$

12: Verify convergence criteria: $\eta < tol$

Moreover, the case of matching meshes on the interface between auxiliary and local models is assumed. For the case of non-matching meshes, a projection step needs to be developed to communicate the displacement field from the global to the local model, and the reaction forces from the local to the global auxiliary domain.

This algorithm is no more than a fixed point for which the convergence is known to be slow. Full linear models can be considered as preconditioners for a Krylov solver to improve the convergence rate. In the case of a non-linear local model, quasi-Newton or Aitken's relaxation must be taken into account [11, 18].

3 Global/Local method with Robin Parameters

As previously stated, the standard global/local analysis can be observed as a coupling of the complementary and local model by means of a Lagrange's multiplier. This coupling problem can be solved with an iterative Dirichlet-

Neumann fixed-point algorithm.

115 However, in the same way as Schwarz domain decomposition methods [14], Robin conditions can be introduced to enhance the convergence and obtain more flexibility. In fact, the kinematic compatibility between the complementary and local model is broken and replaced by Robin conditions written on the interface Γ . The first studies in the global/local method with Robin conditions are introduced in [15] and reminded in [18]. The proposal in this paper is to go further and derive a complete mixed global/local method.

120 3.1 Derivation of Global/Local Analysis with Robin Parameters

The mechanical problem is presented differently in this section as it follows a mixed domain decomposition framework. Instead of using a Lagrange's multiplier specified on the interface Γ , reaction forces $\boldsymbol{\lambda}_L$ and $\boldsymbol{\lambda}_C$ are considered as full unknowns on the interface. The conditions to be enforced at the interface are provided by writing the problem as a domain decomposition:

$$\begin{aligned} \boldsymbol{\lambda}_L + \boldsymbol{\lambda}_C &= 0 && \text{Equilibrium of forces} \\ \mathbf{C}_L \mathbf{u}_L - \mathbf{C}_C \mathbf{u}_C &= 0 && \text{Continuity of displacements} \end{aligned} \quad (17)$$

These two equations interpreting the interface behaviour are written with Robin conditions:

$$\begin{aligned} \boldsymbol{\lambda}_L + \boldsymbol{\lambda}_C - \mathbf{k}_C (\mathbf{C}_L \mathbf{u}_L - \mathbf{C}_C \mathbf{u}_C) &= 0 \\ \boldsymbol{\lambda}_L + \boldsymbol{\lambda}_C + \mathbf{k}_L (\mathbf{C}_L \mathbf{u}_L - \mathbf{C}_C \mathbf{u}_C) &= 0 \end{aligned} \quad (18)$$

125 \mathbf{k}_C and \mathbf{k}_L are Robin parameters, which are stiffness operators. Symmetric definite positive operators are selected to ensure the equivalence with Eq. (17) of the interface. These Robin conditions are determined and written on the interfaces, connecting reaction forces $\boldsymbol{\lambda}_C$ and $\boldsymbol{\lambda}_L$ to the interface displacements $\mathbf{C}_L \mathbf{u}_L$ and $\mathbf{C}_C \mathbf{u}_C$.

Thus, the new system to be solved is:

$$\begin{aligned} \mathbf{K}_C \mathbf{u}_C &= \mathbf{f}_d^C + \mathbf{C}_C^T \boldsymbol{\lambda}_C \\ \boldsymbol{\lambda}_L + \boldsymbol{\lambda}_C - \mathbf{k}_C (\mathbf{C}_L \mathbf{u}_L - \mathbf{C}_C \mathbf{u}_C) &= 0 \\ \mathbf{K}_L \mathbf{u}_L &= \mathbf{f}_d^L + \mathbf{C}_L^T \boldsymbol{\lambda}_L \\ \boldsymbol{\lambda}_L + \boldsymbol{\lambda}_C + \mathbf{k}_L (\mathbf{C}_L \mathbf{u}_L - \mathbf{C}_C \mathbf{u}_C) &= 0 \end{aligned} \quad (19)$$

130 Similarly, as the standard global/local method, the problem in the complementary model is generalized to the global model. Therefore, the first equation of the system becomes as follows:

$$\mathbf{K}_G \mathbf{u}_G = \mathbf{f}_d^G + \mathbf{C}_G^T \boldsymbol{\lambda}_C + \mathbf{C}_G^T \boldsymbol{\lambda}_A \quad (20)$$

In addition, as \mathbf{u}_G and \mathbf{u}_C are equal on the interface Γ , Robin conditions can also be written as:

$$\begin{aligned} \boldsymbol{\lambda}_L + \boldsymbol{\lambda}_C - \mathbf{k}_G (\mathbf{C}_L \mathbf{u}_L - \mathbf{C}_G \mathbf{u}_G) &= 0 \\ \boldsymbol{\lambda}_L + \boldsymbol{\lambda}_C + \mathbf{k}_L (\mathbf{C}_L \mathbf{u}_L - \mathbf{C}_G \mathbf{u}_G) &= 0 \end{aligned} \quad (21)$$

with $\mathbf{k}_G = \mathbf{k}_C$.

Remark 2. $\boldsymbol{\lambda}_C$ is the reaction force of a problem in the complementary domain. Therefore, it is preferable not to use the notation $\boldsymbol{\lambda}_G$ in order to avoid a confusion on the nature of $\boldsymbol{\lambda}_G$.

135 The first equation of the Robin conditions allows to obtain the expression of $\boldsymbol{\lambda}_C$ to incorporate it into the equilibrium of the global model, which led to:

$$\mathbf{K}_G \mathbf{u}_G = \mathbf{f}_d^G + \mathbf{C}_G^T \boldsymbol{\lambda}_A - \mathbf{C}_G^T (\boldsymbol{\lambda}_L - \mathbf{k}_G \mathbf{C}_L \mathbf{u}_L - \mathbf{k}_G \mathbf{C}_G \mathbf{u}_G) \quad (22)$$

The second equation of the Robin conditions allows to obtain the expression of $\boldsymbol{\lambda}_L$ to incorporate it into the equilibrium of the local model, which led to the following equation:

$$(\mathbf{K}_L + \mathbf{C}_L^T \mathbf{k}_L \mathbf{C}_L) \mathbf{u}_L = \mathbf{f}_d^L + \mathbf{C}_L^T (\mathbf{k}_L \mathbf{C}_G \mathbf{u}_G - \boldsymbol{\lambda}_C) \quad (23)$$

Similarly as the global/local method, a fixed-point algorithm can be derived where an iteration consists of the following steps:

1. Global problem: knowing $(\mathbf{u}_L^n, \lambda_L^n, \lambda_A^n)$, find \mathbf{u}_G^{n+1} solution of:

$$\mathbf{K}_G \mathbf{u}_G^{n+1} = \mathbf{f}_d^G + \mathbf{C}_G^T \underbrace{(\lambda_A^n - (\lambda_L^n - \mathbf{k}_G \mathbf{C}_L \mathbf{u}_L^n - \mathbf{k}_G \mathbf{C}_G \mathbf{u}_G^n))}_{\mathbf{P}^n} \quad (24)$$

2. Auxiliary problems: computing the reaction forces on Ω_A and Ω_C on the interface Γ :

$$\begin{aligned} \lambda_A^{n+1} &= \mathbf{C}_A (\mathbf{K}_A \mathbf{u}_G|_{\Omega_A} - \mathbf{f}_d^A) \\ \lambda_C^{n+1} &= \mathbf{C}_C (\mathbf{K}_C \mathbf{u}_G|_{\Omega_C} - \mathbf{f}_d^C) \end{aligned} \quad (25)$$

3. Local problem: knowing $(\mathbf{u}_G^{n+1}, \lambda_C^{n+1})$, find \mathbf{u}_L^{n+1} solution of:

$$(\mathbf{K}_L + \mathbf{C}_L^T \mathbf{k}_L \mathbf{C}_L) \mathbf{u}_L^{n+1} = \mathbf{f}_d^L + \mathbf{C}_L^T (\mathbf{k}_L \mathbf{C}_G \mathbf{u}_G^{n+1} - \lambda_C^{n+1}) \quad (26)$$

Remark 3. As to preserve the global model without any change, the contribution of \mathbf{u}_G is considered on the right-hand side of the previous equation with the term $-\mathbf{C}_G^T \mathbf{k}_G \mathbf{C}_G \mathbf{u}_G^n$, due to the Robin parameter \mathbf{k}_G . In fact, the contribution of Robin conditions leads to local changes of global stiffness operators regarding the interface degrees of freedom. For another framework of dealing with Robin conditions see [30]

As mentioned in the previous section, auxiliary problems are not needed if finite element codes can get reaction forces on an immersed surface. Nevertheless, if this is not the case, the auxiliary problem in Ω_C is still not necessary. Indeed, it can be computed from known and easy computations without assembling the operator \mathbf{K}_C :

$$\begin{aligned} \lambda_C^{n+1} &= \mathbf{C}_C (\mathbf{K}_C \mathbf{u}_G^{n+1}|_{\Omega_C} - \mathbf{f}_d^C) \\ &= \mathbf{C}_G (\mathbf{K}_G \mathbf{u}_G^{n+1} - \mathbf{f}_d^G - (\bar{\mathbf{K}}_A \mathbf{u}_G^{n+1} - \bar{\mathbf{f}}_d^A)) \\ &= \mathbf{C}_G \mathbf{C}_G^T \mathbf{P}^n - \lambda_A^{n+1} \\ \lambda_C^{n+1} &= \mathbf{P}^n - \lambda_A^{n+1} \end{aligned} \quad (27)$$

The same relation as the standard global/local method is given where $\mathbf{P}^n = \lambda_C^{n+1} + \lambda_A^{n+1}$. In addition, since $\mathbf{P}^n = \lambda_A^n - \lambda_L^n + \mathbf{k}_G \mathbf{C}_L \mathbf{u}_L^n - \mathbf{k}_G \mathbf{C}_G \mathbf{u}_G^n$, \mathbf{P}^{n+1} can be written in function of \mathbf{P}^n , a new rest \mathbf{r}^{n+1} will appear:

$$\begin{aligned} \mathbf{P}^{n+1} &= \lambda_A^{n+1} - \lambda_L^{n+1} + \mathbf{k}_G \mathbf{C}_L \mathbf{u}_L^{n+1} - \mathbf{k}_G \mathbf{C}_G \mathbf{u}_G^{n+1} \\ &= \mathbf{P}^n - \lambda_C^{n+1} - \lambda_L^{n+1} + \mathbf{k}_G \mathbf{C}_L \mathbf{u}_L^{n+1} - \mathbf{k}_G \mathbf{C}_G \mathbf{u}_G^{n+1} \\ &= \mathbf{P}^n - [(\lambda_C^{n+1} + \lambda_L^{n+1}) + \mathbf{k}_G (\mathbf{C}_G \mathbf{u}_G^{n+1} - \mathbf{C}_L \mathbf{u}_L^{n+1})] \\ &= \mathbf{P}^n + \mathbf{r}^{n+1} \end{aligned} \quad (28)$$

The new rest \mathbf{r}^{n+1} now incorporates a mixed contribution of the discontinuity of displacements and the disequilibrium of forces:

$$\mathbf{r}^{n+1} = \underbrace{-(\lambda_C^{n+1} + \lambda_L^{n+1})}_{\text{Disequilibrium}} - \underbrace{\mathbf{k}_G (\mathbf{C}_G \mathbf{u}_G^{n+1} - \mathbf{C}_L \mathbf{u}_L^{n+1})}_{\text{discontinuity}} \quad (29)$$

3.2 Algorithm for Global/Local method with Robin Parameters

The mixed global/local methodology with Robin conditions can be located in Alg. 2.

Algorithm 2 Global/Local algorithm with Robin Conditions

1: Initialize interface vector $\mathbf{P}^0 = 0$

2: Initialize error $\eta = 1$ and tolerance tol

3: Start iterations, $n = 0$

4: **while** $\eta > tol$ **do**

5: Solve the global problem:

$$\text{Find } \mathbf{u}_G^{n+1}, \mathbf{K}_G \mathbf{u}_G^{n+1} = \mathbf{f}_d^G + \mathbf{C}_G^T \mathbf{P}^n$$

6: Solve the auxiliary problem:

$$\text{Find } (\mathbf{u}_A, \boldsymbol{\lambda}_A^{n+1}), \begin{bmatrix} \mathbf{K}_A & \mathbf{C}_A^T \\ \mathbf{C}_A & 0 \end{bmatrix} \begin{bmatrix} \mathbf{u}_A \\ -\boldsymbol{\lambda}_A^{n+1} \end{bmatrix} = \begin{bmatrix} \mathbf{f}_d^A \\ \mathbf{u}_G^{n+1} |_{\Gamma} \end{bmatrix}$$

7: Compute the reaction force $\boldsymbol{\lambda}_C^{n+1}$:

$$\boldsymbol{\lambda}_C^{n+1} = \mathbf{P}^n - \boldsymbol{\lambda}_A^{n+1}$$

8: Solve the local problem:

$$\text{Find } \mathbf{u}_L^{n+1},$$

$$(\mathbf{K}_L + \mathbf{C}_L^T \mathbf{k}_L \mathbf{C}_L) \mathbf{u}_L^{n+1} = \mathbf{f}_d^L + \mathbf{C}_L^T (\mathbf{k}_L \mathbf{C}_G \mathbf{u}_G^{n+1} - \boldsymbol{\lambda}_C^{n+1})$$

9: Compute the reaction force $\boldsymbol{\lambda}_L^{n+1}$:

$$\boldsymbol{\lambda}_L^{n+1} = -\boldsymbol{\lambda}_C^{n+1} - \mathbf{k}_L (\mathbf{C}_L \mathbf{u}_L^{n+1} - \mathbf{C}_G \mathbf{u}_G^{n+1})$$

10: Compute the residual of the iteration $\mathbf{r}^{n+1} = -[(\boldsymbol{\lambda}_C^{n+1} + \boldsymbol{\lambda}_L^{n+1}) + \mathbf{k}_G (\mathbf{C}_G \mathbf{u}_G^{n+1} - \mathbf{C}_L \mathbf{u}_L^{n+1})]$

11: Compute the new \mathbf{P}^{n+1} :

$$\mathbf{P}^{n+1} = \mathbf{P}^n + \mathbf{r}^{n+1}$$

12: Update the new \mathbf{P}^{n+1} including relaxation factor μ :

$$\mathbf{P}^{n+1} = \mu \mathbf{P}^{n+1} + (1 - \mu) \mathbf{P}^n$$

13: Estimate the error of the iteration step as $\eta = \|\mathbf{r}^{n+1}\|_2 / \|\mathbf{r}^0\|_2$

14: Verify convergence criteria: $\eta < tol$ with $tol = 10^{-4}$

The method error is calculated by using the same expression as for the primal-dual strategy presented in Eq. (16). However, each residual term in Eq. (16) is calculated differently for the mixed global/local analysis (it is estimated as a combination of interface forces and displacements). It could be interesting to take into consideration the error of the results reached when using the global/local analysis with mixed conditions and the results regarding the monolithic computation. This error is calculated as the rule of displacement difference on the interface between the global and the monolithic model, as presented in Eq. (30).

$$\eta_{Mono.} = \frac{\|(\mathbf{C}_G \mathbf{u}_G^{n+1} - \mathbf{u}_{Mono.})\|_2}{\|\mathbf{u}_{Mono.}\|_2} \quad (30)$$

Figure 3 shows a flowchart of the iterative method implementation of the global/local with Robin parameters.

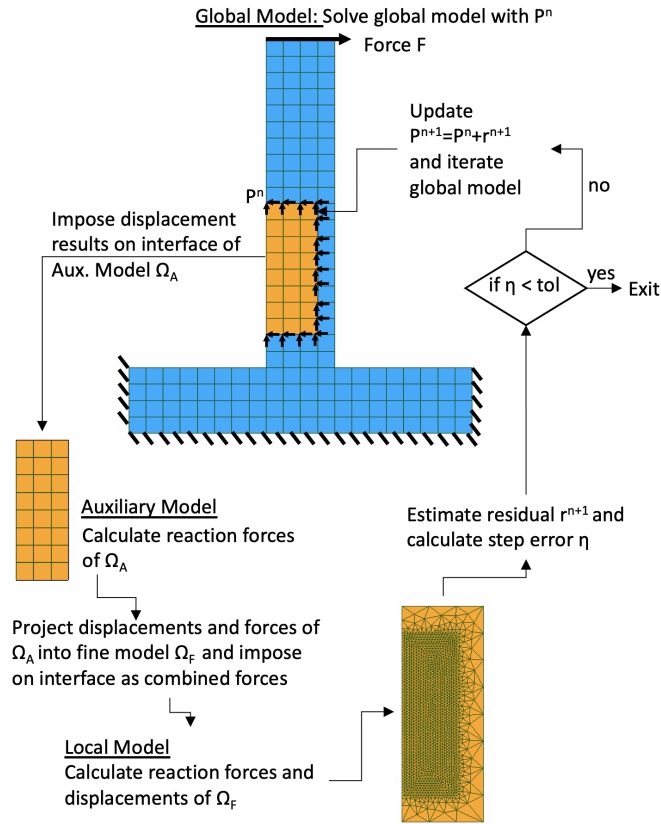


Figure 3: Flowchart of the algorithm of the Global/Local Analysis with Robin Parameters.

4 Results for 2D structures using Global/Local Analysis with Robin Parameters

4.1 Description of the two cases - definition of the Robin Parameters

165 *Code Aster* [12] was used to implement the global/local algorithm with Robin parameters as two A-36 steel structures modelled with 2D plane stress formulation: a) an inverted T-Shape with a 10mm initial crack and b) an inverted T-Shape model with a circular cut to induce the plastic hardening behaviour. The properties used for the analysis correspond to: Yield stress of 250 (MPa), hardening ratio of 0.1 and 4 propagation steps with a maximum advance of 2 (mm) per step. Geometrical properties are presented in Figure 4a and Figure 4b.

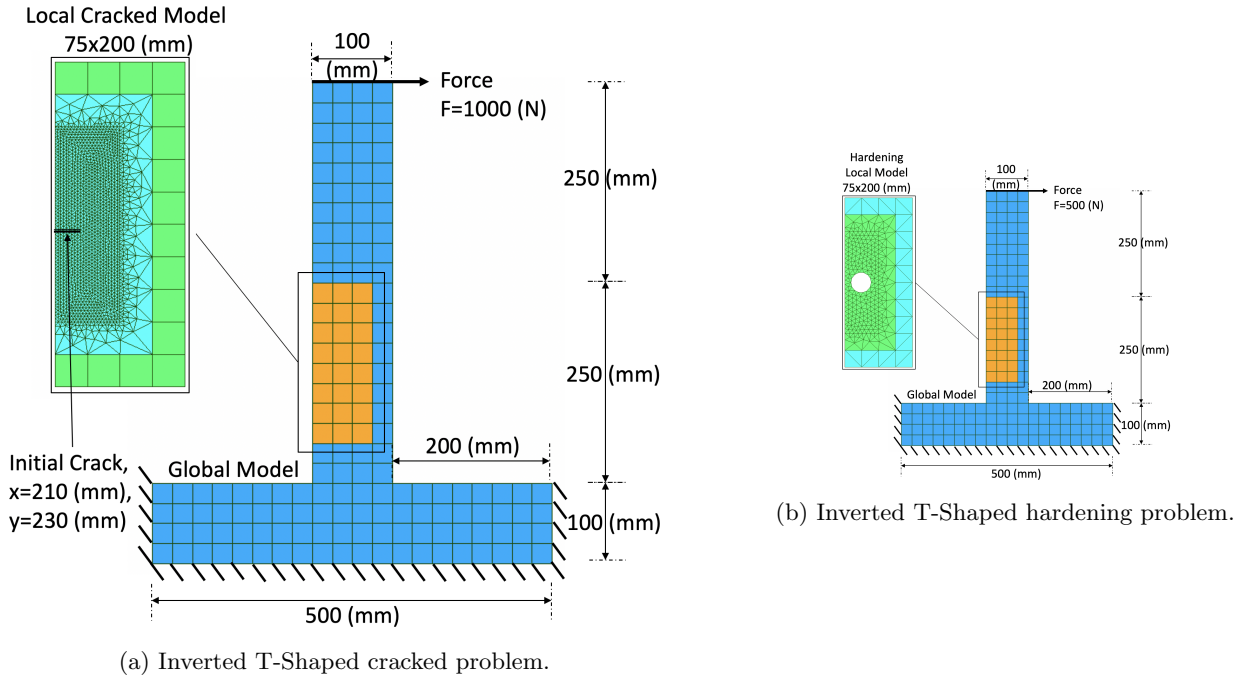


Figure 4: Geometry of analyzed models.

The Robin parameter is chosen as the stiffness of an element strip [33], as presented in Figure 5. Robin operators \mathbf{k}_L and \mathbf{k}_G are determined independently: \mathbf{k}_L is the linear elastic stiffness of the strip on the side of the complementary model from the interface and \mathbf{k}_G is the linear elastic stiffness of the strip on the side of the local model from the interface. In addition, Aitken's δ^2 dynamic relaxation is used to accelerate the convergence in relation to a classical static relaxation.

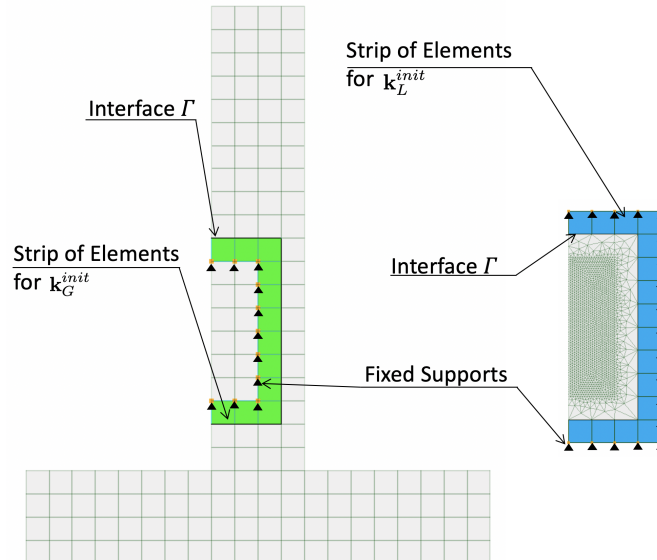


Figure 5: Element strip of elements used for the analysis.

Remark 4. In the Code Aster implementation, the Robin operator is calculated as follows: the strip of elements is

175 applied with a Young Modulus variable ($\alpha_L E_L$) for the local model, modifying the stiffness and considering coupled
degrees of freedom on the interface. This strip of elements is connected directly to the interface and with fixed
support boundary conditions. On the other hand, the strip of elements is used to compute the part on the right-hand
side for the global model, which corresponds to the Robin conditions in Eq. (28). It is not assembled with the global
180 stiffness. The strip of elements considers a Poisson ratio of 0.3, a Young Modulus variable ($\alpha_G E_G$) and fixed
boundary conditions on the opposite side of the interface, as presented in Figure 5.

4.2 Results

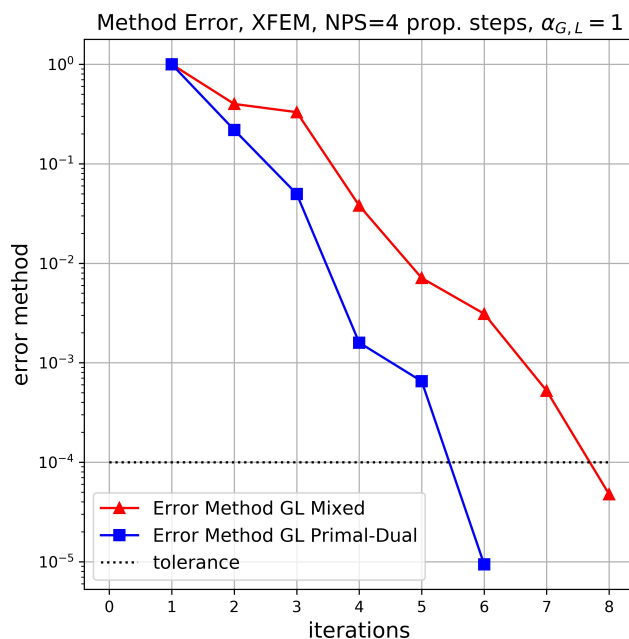


Figure 6: Method error for Global/Local Analysis with Robin Parameters and cracked domain with 4 propagation steps.

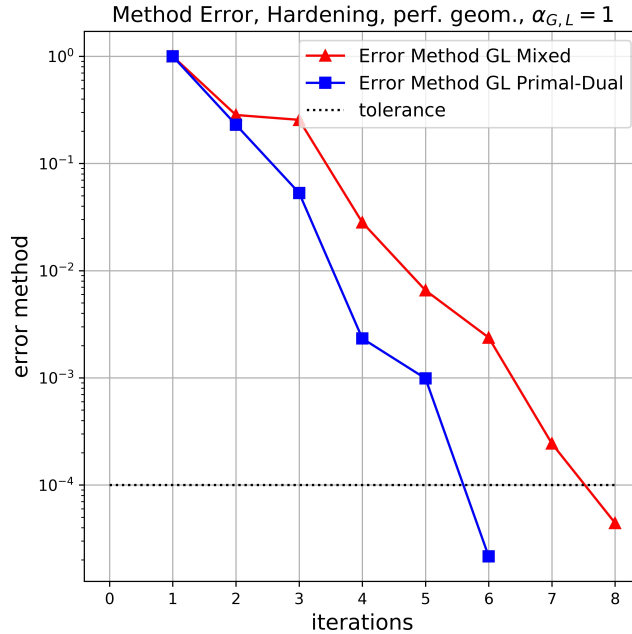


Figure 7: Method error for Global/Local Analysis with Robin Parameters and plastic hardening domain.

It is clear that the global/local Analysis with Robin parameters converges slower with respect to the primal-dual Method (from 8 to 6 iterations compared to the primal-dual for the cracked model). For the hardening problem, it converges from 8 to 6 with respect to the primal-dual and considering the number of iterations. The Aitken δ^2 dynamic relaxation converges both models rapidly, with a faster convergence rate for the primal-dual Method.

The complete global/local analysis results with the initial Robin operator are shown in Table 1 for non-linear/cracked behaviour.

Model	Mono. Error	Method Error	Iter. for Conv.
Cracked	6.9E-06	4.7E-05	8
Hardening	6.0E-06	4.4E-05	8

Table 1: Results for both models and non-linear/cracked behaviour, using Aitken δ^2 and the Initialized Robin Operator.

Summary of the Results

As presented in Section 4, the mixed method converges slower with respect to the primal-dual method. Regarding computational times, these were 18 seconds for the cracked model and 10 seconds for the non-linear hardening problem. However, these times are referential and can be improved by optimizing the python code. Finally, as the analysis considers an arbitrary strip of elements used to start the Robin operator, an optimization process is carried out with the intention of reducing the number of iterations until convergence and analysing the results for different Robin parameter values. In addition, the strip of elements are very stiff and do not represent the neighbour structure, i.e., the theoretical optimum.

Remark 5. *Is important to mention that non-linear plastic behaviour or crack tip propagation are not being transferred between the local and global models. The interfaces are considered far from the source of plasticity or the*

200 crack tip; Therefore, based on St. Venant’s principle, only the effects of these singularities are transmitted between models. In order to study specific aspects of the non-linear behaviour, the local model should be further analyzed. Finally, the ”total” solution of the analysis should be considered as the superposition of the global linear model and the local non-linear model.

205 5 Optimization of the Robin parameter Global/Local Analysis with Robin Conditions in 2D plane stress

5.1 Description of the optimization process

As presented in [25], the convergence of the global/local analysis with mixed conditions can be assured for a certain range of values for the Robin parameters. Within this range, an optimum that minimizes the number of iterations can be found. However, as presented in [34, 13], the value depends on the problem type, the applied loads, the boundary conditions and the form of the Robin operator used in the analysis. Therefore, in order to find the Robin operator that guarantees convergence and also minimizes the number of iterations until convergence, an optimization process is performed for the different problems presented. Optimization algorithms have been used widely in engineering problems and other scientific areas, such as the Basin-Hopping Algorithm [24, 29], already distributed within Scipy library [36].

215 **Remark 6.** *The values of the Robin operator assuring the convergence of the non-intrusive method with Robin conditions can be estimated analytically for simple examples with few degrees of freedom. For industrial/real structures, the range of the values are not easily found directly, so these values are found by iterative methods as presented in [20, 13] or by using two scale strategies as shown in [27, 15].*

For this article, the Basin-Hopping algorithm is used in the optimization process, allowing the specification of an initial “guess” of the problem within the search space and stochastically start the refinement of the solution until finding the best possible solution. The Basin-Hopping algorithm is based on the transformation of the ”potential energy landscape” of an objective function, finding local minima using the Limited-Memory Broyden-Fletcher-Goldfarb-Shanno method (L-BFGS) [9]. This potential energy surface is being explored by means of random jumps for each evaluation based on the Boltzmann probability distribution. The number of random jumps is defined by a variable N, in which the probabilities for finding the best local minimum are increased for larger values of N. Therefore, the Basin-Hopping algorithm has been used successfully to find a minimum using N=110 or larger [37]. This parameter is also a measurement of the computational cost, because it is a direct measurement of the amount of random jumps between each solution. For our work, N has been defined as the default option provided in Scipy, with a value of N equal to 100. Finally, the L-BFGS method has a computational complexity of $\mathcal{O}(n^2)$ and must be repeated N times in accordance with the number of random jumps [8].

Nevertheless, a global optimum cannot be assured in metaheuristics, due to the non-convex nature of the problem. However, a good approximation of a global minimum solution can be found. This is due to the internal behaviour of the optimization process: it is stopped through an internal convergence criterion and not by founding a global minimum [3]. More information and applications on the different optimization algorithms can be seen in [10, 21, 2, 22, 26, 7, 40, 35], among others. Therefore, considering that the convergence of the method depends on the Robin parameters as presented in [25], the initial Robin parameter (calculated as the condensed stiffness on the interface estimated from an initial strip of elements and presented in Figure 5) can be modified by means of two factors: α_G for the global model and α_L for the local fine model, as shown in Eq. (31):

$$\mathbf{k}_L = \alpha_L \mathbf{k}_L^{init} \quad \mathbf{k}_G = \alpha_G \mathbf{k}_G^{init} \quad (31)$$

The optimization algorithm will be used to find an optimum value for $\alpha_{G,L}$ that minimizes the number of iterations until convergence.

It is important to note that the search space for the values of $\alpha_{G,L}$ to be used in the optimization process are constrained between 0 and 100 in order to find an overall optimum that minimizes the number of iterations, starting with the initial search direction $\mathbf{k}_{G,L}^{init}$, i.e., $\alpha_G = 1$ and $\alpha_L = 1$.

245 The optimization problem is carried out using the initial configuration of the domains and considering the initialized Robin conditions and multiplied by the α factor. The analysis contemplates linear elasticity behaviour for both problems for all optimization trials. Finally, the results for the optimum $\alpha_{G,L}$ will be used for non-linear problems (all propagation steps and post-yielding hardening).

The following procedure is applied to perform the optimization of the Robin parameter, using the Basin-Hopping [29] algorithm, as well as for linear elastic initialized models, i.e., without plasticity or crack propagation:

- 250 • Choose global and local models to be analysed considering the elastic linear behaviour, as presented in Figure 4a and Figure 4b.
- Perform the analysis on the model considering the iterative non-intrusive scheme with $\alpha_L = 1$ and $\alpha_G = 1$ (Initial guess or initial trial for the Robin parameter).
 1. Choose new values of α_L and α_G found in the local neighbourhood of the initial guess.
 - 255 2. Perform the non-intrusive analysis using Robin parameters and recover the number of iterations until the analysis converges for each α_L and α_G in the neighbourhood of the current trial.
 3. Study the convergence values of the previous neighbourhood and select random values in the best direction (gradient) found in the neighbour to proceed with updated $\alpha_{G,L}$ trial.
- When the optimization algorithm converges and the best solution for the linear model is obtained, the best factors α_L^{opt} and α_G^{opt} are recovered.
- 260 • Apply α_L^{opt} and α_G^{opt} to the non-linear model (hardening or cracked model) and study the convergence.

5.2 Results

For the 2D cases, the optimization results are presented summarized in Table 2 for both models.

Model	(α_G, α_L)	Mono. Error	Method Error	Iter. Conv.
Init. cracked	(1.167,4.353)	6.1E-06	9.8E-05	5
Init. perforated	(0.515,1.676)	3.4E-06	8.7E-05	7

Table 2: Optimized α results for initial cracked and perforated linear model.

265 The optimized α found for the linear cases are used directly as an input for the non-linear cases. These results, regarding the evolution of the method error with respect to iterations, are introduced in Figure 8 for the cracked case and in Figure 9 for the plastic hardening case.

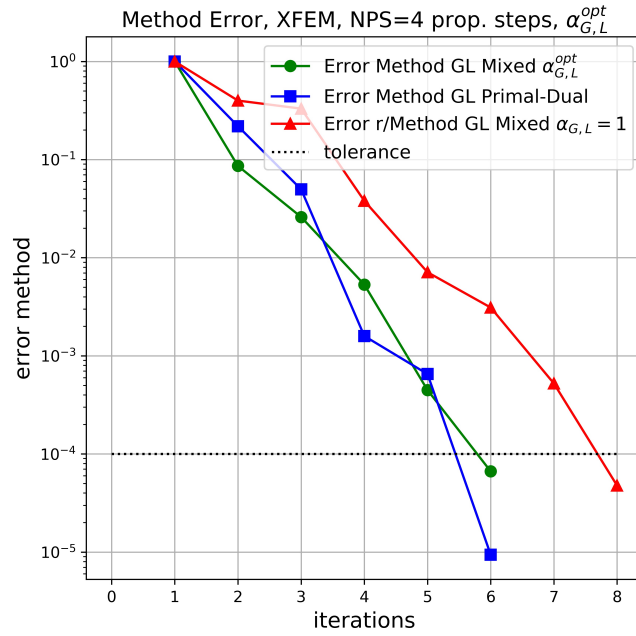


Figure 8: Method error for Global/Local Analysis with Optimized Robin Parameters and cracked domain.

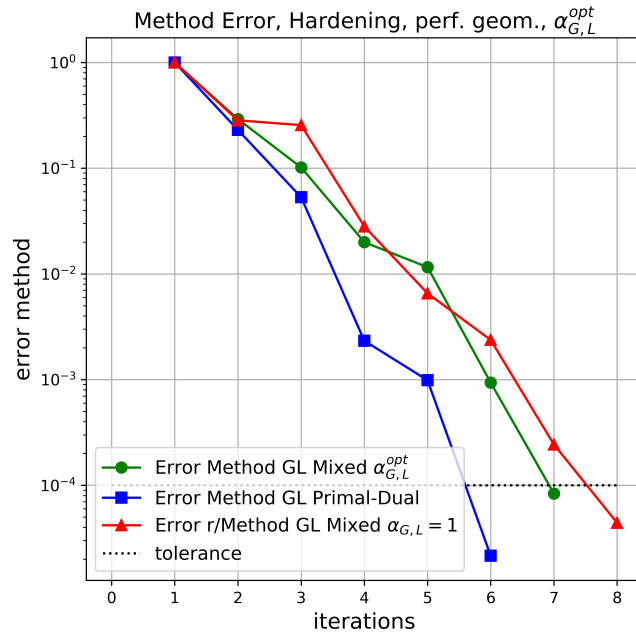


Figure 9: Method error for Global/Local Analysis with Optimized Robin Parameters and plastic hardening domain.

Figure 8 and Figure 9 show that the number of iterations are reduced by 25% for the cracked case and 12.5% for the plastic hardening case respecting the non-optimized solution (initial guess of the Robin parameter). However, with regard to the primal-dual solution, the cracked optimized model equals the performance in terms of the number of iterations. For the non-linear hardening case, the optimized model with Robin parameters performs slower with respect to the primal-dual method. The results for the cracked model and non-linear hardening, using the optimized $\alpha_{G,L}$ factors, are presented in Table 3.

Model	(α_G, α_L)	Mono. Error	Method Error	Iter. Conv.
Cracked	(1.167 , 4.353)	4.3E-06	6.6E-05	6
Hardening	(0.515 , 1.676)	2.4E-06	8.3E-05	7

Table 3: Results for optimized α , cracked behaviour (4 propagation steps) and post-yielding hardening.

Summary of the Results

When optimizing the linear elastic analysis of each model (including the initial configuration of the local geometry) using the Basin-Hopping algorithm, the convergence of non-linear models is improved as expected. The optimized α_L^{opt} and α_G^{opt} used for the non-linear problems obtain better results with respect to the non-optimized problems, similar to the performance of the primal-dual method. This approximation using the linear elastic optimized model works for localized patches with non-linearities. However, the solution found with the Basin-Hopping algorithm for the linear models may not be the actual optimum for the non-linear models. Finally, as the Code Aster code with the python interface was implemented, the optimization times are elevated in comparison with the non-optimized α case. However, these times can be optimized by using better coding practices and more efficiency in computing resources.

6 Global/Local Analysis with Robin Conditions for 3D structures

As presented in Section 5, the same approach will be applied in two models: a cantilever beam with an initial crack near the fixed support and a beam with two 50 (mm) perforations and non-linear hardening behaviour. The properties are the same as the previous case but including different lengths, loads applied and crack size, as shown in Figure 10. The crack propagates for the 3D case, including 3 propagation steps and 10 (mm) for maximum crack advance per step for the cracked domain.

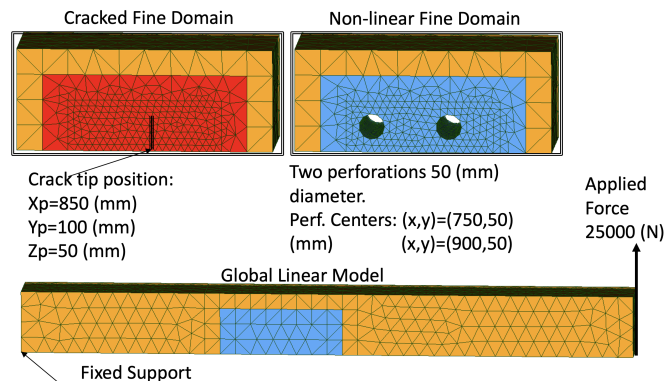


Figure 10: 3D cantilever cracked and non-linear hardening beam.

As the discretization carried out in the global and local 3D models are geometrically complex, incompatible meshes were generated. The incompatibility is managed by *Code Aster* projecting the fields between the models

and the interface. The initial Robin parameter will be used in order to find the results for the non-optimized $\alpha_{G,L}$ for both models, which are summarized in Table 4.

Model	(α_G, α_L)	Mono. Error	Method Error	Iter. Conv.
Cracked	(1, 1)	0.437	5.19E-05	10
Hardening	(1, 1)	0.371	4.53E-05	10

Table 4: Results for the optimization for 3D model with initial conditions and linear behaviour.

295 Results using the optimized Robin parameter, following the same procedure as shown in Sec. 5, are summarized in Table 5 and presented in Figure 11 for the cracked case and in Figure 12 for the plastic hardening case.

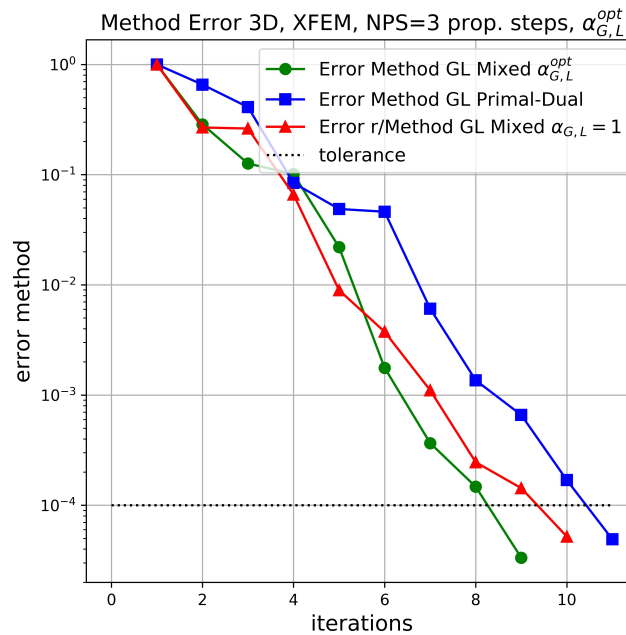


Figure 11: Method error for Global/Local Analysis Robin Parameters for 3D cracked domain and optimized $\alpha_{G,L}$.

300 The use of the optimized $\alpha_{G,L}$ implies a reduction on the number of iterations from 10 to 9 for the cracked case with 3 propagation steps, meaning a 18% faster respect to the primal-dual and a 10% improvement in relation to the global/local with non-optimized Robin conditions. For the hardening problem, the optimized $\alpha_{G,L}$ reduces the number of iterations from 10 to 8, which corresponds to an improvement of 20% with respect to the non-optimized Robin conditions and 11% improvement in comparison to the primal-dual solution. The complete results for the 3D analysis are presented in Table 5.

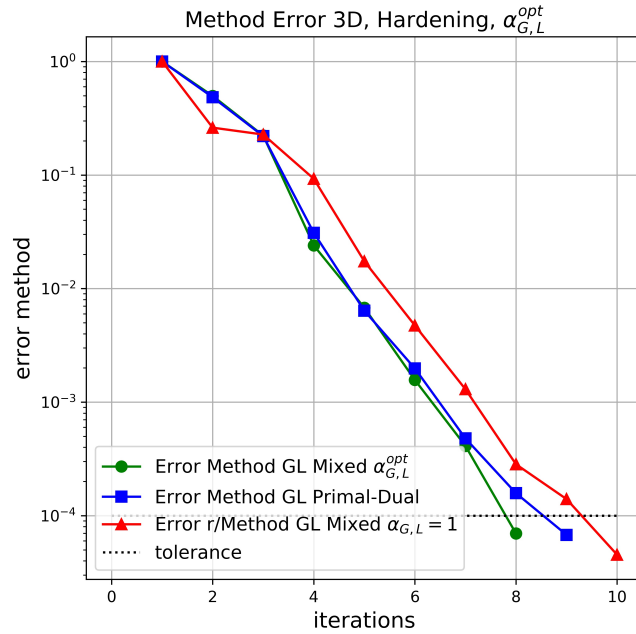


Figure 12: Method error for Global/Local Analysis Robin Parameters for 3D hardening domain and optimized $\alpha_{G,L}$.

Model	(α_G, α_L)	Mono. Error	Method Error	Iter. Conv.
Cracked	(1.39 , 2.31)	0.727	3.34E-05	9
Hardening	(0.386 , 1.840)	0.311	6.96E-05	8

Table 5: Results for the 3D cracked models 3 propagation steps.

The final deformed shape for the cracked model is presented in Figure 13 for the Global/Local 3D model with Robin conditions (optimized) and in Figure 14 for the hardening case.

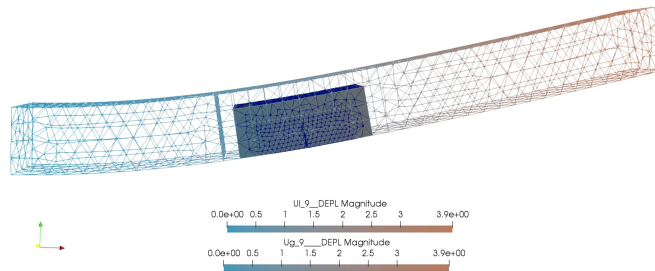


Figure 13: Deformed shape of the 3D beam for Global/Local Analysis with Optimized Robin Parameters and cracked domain.

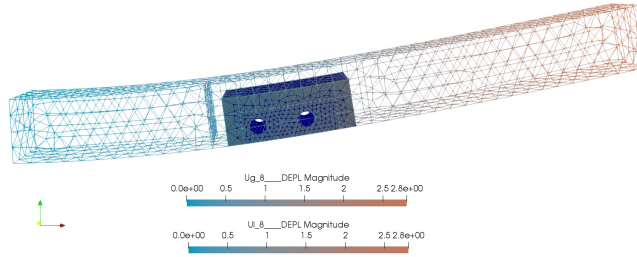


Figure 14: Deformed shape of the 3D beam for Global/Local Analysis with Optimized Robin Parameters and hardening domain.

Summary of the Results

As in Section 5, the optimization improves the convergence with respect to the initialized Robin parameter.

The optimization process, when applied to the 3D cracked model, improves the convergence rate, resulting in better performances, considering the number of iterations with respect to the primal-dual methodology.

7 Discussion

In this article, the global/local non-intrusive analysis with Robin parameters was implemented in 2D and 3D problems with cracked and plastic hardening behaviour. Subsequently, results were optimized using the Basin-Hopping algorithm and compared to a primal-dual non-intrusive analysis.

The method presented in this study has a good convergence rate for 2D and 3D non-linear plastic hardening behaviour and cracked models. However, as for any mixed method, the selection of the Robin parameters is crucial for convergence. Our initial choice is based on studying the effect of a simple element strip, but it may not be very efficient compared to the primal-dual approach.

The optimization of the mixed global/local method was performed using the Basin-Hopping algorithm, allowing an improvement in the performance of the global/local analysis with Robin parameters. The optimized α is different for each case, which is consistent with results presented in [34], indicating that the values of α are specific to each model (geometry, behaviour, etc.), loads and boundary conditions.

Nevertheless, the optimization does not guarantee that the mixed global/local analysis works better with respect to the primal-dual non-intrusive analysis, although a local minimum could improve the mixed analysis results.

8 Future research

The Robin parameter and the flexibility added to the structure are a great advantage of the mixed model, as presented in [20]. Therefore, the non-intrusive analysis with Robin parameters can be studied for structures with geometric non-linear behaviour and large displacements.

Another topic to be studied further is to extend the analysis to larger structures, associated with multiple domains and with multiple stiffeners or variable cross sections. This is useful to study the convergence of the method in structures with strong modifications in the stiffness. Consequently, the original approximation of the Robin parameter may not be the best for each interface and these factors could be different for each analysis direction, as presented in [13].

Different crack propagation techniques must be considered in future studies, for example, the Cohesive Zone Model (CZM) and the Virtual Closing-Crack Technique (VCCT) to study the effectiveness of the global/local

method with Robin parameters using this type of analysis. The feasibility of coupling the global/local method with phase field approaches to deal with crack propagation has been studied successfully in [17, 28].

The studied strategies for solving the global/local problem, i.e., primal-dual and with Robin conditions, work without problems for incompatible patches. Nevertheless, a sensitivity analysis can be performed to study the effect of incompatible meshes for different structures and behaviours, and the error that can be induced due the interpolation of forces and displacements in the different interfaces.

Basin-Hopping is a meta-heuristic that can be easily implemented, but as presented in [5], it may not be the fastest to obtain convergence. Therefore, a more efficient way to optimize the Robin parameters and reduce computational times must be studied and applied, such as the Particle Swarm Optimization [39] and exploiting the ability to evaluate multiple trials with parallel architecture. In addition, the efficiency of the algorithm on larger cases will be studied. For now, due to the small problems we studied, the iterative algorithm cannot compete with a full-scale computation. We expect that larger problems may reverse this trend.

Finally, the effect of the discretization for the 2D and 3D models, the degree of the shape functions used for the FEM method elements and also the coupling between 2D global models and 3D local non-linear models must be analyzed, in order to study the convergence of these elements and how affects the response.

9 Acknowledgements

This work was partly funded by the international project ECOS-CONICYT C17E04 between LMT and Universidad de Talca, ANID/CONICYT grant number ECOS C17E04. In addition, this research was funded by ANID, grant number PFCHA / DOCTORADO BECAS CHILE / 2018 - 21181707 and BECA ESTUDIO DE DOCTORADO, UNIVERSIDAD DE TALCA

Conflict of interest

The authors declare that they have no conflict of interest.

References

- [1] F. Aldakheel, N. Noii, T. Wick, and P. Wriggers. A global–local approach for hydraulic phase-field fracture in poroelastic media. *Computers & Mathematics with Applications*, 91:99–121, 6 2021.
- [2] B. V. Babu and M. M. Jehan. Differential evolution for multi-objective optimization. In *2003 Congress on Evolutionary Computation, CEC 2003 - Proceedings*, volume 4, pages 2696–2703. IEEE Computer Society, 2003.
- [3] L. Bianchi, M. Dorigo, L. M. Gambardella, and W. J. Gutjahr. A survey on metaheuristics for stochastic combinatorial optimization. *Natural Computing*, 8(2):239–287, sep 2009.
- [4] M. Blanchard, O. Allix, P. Gosselet, and G. Desmeure. Space/time global/local noninvasive coupling strategy: Application to viscoplastic structures. *Finite Elements in Analysis and Design*, 156:1–12, 2019.
- [5] C. Blum and A. Roli. Metaheuristics in combinatorial optimization: Overview and conceptual comparison. *ACM Comput. Surv.*, 35(3):268–308, Sept. 2003.
- [6] R. Bouclier, J. C. Passieux, and M. Salaün. Local enrichment of NURBS patches using a non-intrusive coupling strategy: Geometric details, local refinement, inclusion, fracture. *Computer Methods in Applied Mechanics and Engineering*, 300:1–26, 2016.
- [7] C. J. Burnham and N. J. English. Crystal Structure Prediction via Basin-Hopping Global Optimization Employing Tiny Periodic Simulation Cells, with Application to Water-Ice. *Journal of Chemical Theory and Computation*, 15(6):3889–3900, jun 2019.

- 375 [8] R. H. Byrd, P. Lu, J. Nocedal, and C. Zhu. A Limited Memory Algorithm for Bound Constrained Optimization. *SIAM Journal on Scientific Computing*, 16(5):1190–1208, sep 1995.
- [9] R. H. Byrd, J. Nocedal, and R. B. Schnabel. Representations of quasi-Newton matrices and their use in limited memory methods. *Mathematical Programming*, 63(1-3):129–156, jan 1994.
- [10] S. Das and P. N. Suganthan. Differential evolution: A survey of the state-of-the-art. *IEEE Transactions on Evolutionary Computation*, 15(1):4–31, 2 2011.
- 380 [11] M. Duval, J.-c. Passieux, M. Salaün, and S. Guinard. Non-intrusive Coupling: Recent Advances and Scalable Nonlinear Domain Decomposition. *Archives of Computational Methods in Engineering*, 23(1):17–38, 3 2016.
- [12] EDF. Code Aster, Analysis of Structures and Thermomechanics for Studies and Research, 2019.
- [13] I. Fuenzalida-Henriquez, J. Hinojosa, L. Peña, and C. Astudillo. Optimizing the search directions of a mixed DDM applied on cracks. *Optimization and Engineering*, 2021.
- 385 [14] M. J. Gander. Schwarz methods over the course of time. *Electronic Transactions on Numerical Analysis*, 31:228–255, 2008.
- [15] L. Gendre, O. Allix, and P. Gosselet. A two-scale approximation of the Schur complement and its use for non-intrusive coupling. *International Journal for Numerical Methods in Engineering*, 87(9):889–905, 9 2011.
- [16] L. Gendre, O. Allix, P. Gosselet, and F. Comte. Non-intrusive and exact global/local techniques for structural 390 problems with local plasticity. *Computational Mechanics*, 44(2):233–245, 2009.
- [17] T. Gerasimov, N. Nohi, O. Allix, and L. De Lorenzis. A non-intrusive global/local approach applied to phase-field modeling of brittle fracture. *Advanced Modeling and Simulation in Engineering Sciences*, 5(1):1–30, 2018.
- [18] P. Gosselet, M. Blanchard, O. Allix, and G. Guguin. Non-invasive global–local coupling as a Schwarz domain decomposition method: acceleration and generalization. *Advanced Modeling and Simulation in Engineering 395 Sciences*, 5(1), 2018.
- [19] G. Guguin, O. Allix, P. Gosselet, and S. Guinard. On the computation of plate assemblies using realistic 3D joint model: a non-intrusive approach. *Advanced Modeling and Simulation in Engineering Sciences*, 3(1):1–23, 2016.
- 400 [20] J. Hinojosa, O. Allix, P. A. Guidault, and P. Cresta. Domain decomposition methods with nonlinear localization for the buckling and post-buckling analyses of large structures. *Advances in Engineering Software*, 70:13–24, 4 2014.
- [21] S. Kukkonen and J. Lampinen. Generalized differential evolution for general non-linear optimization. In *COMPSTAT 2008 - Proceedings in Computational Statistics, 18th Symposium*, pages 459–471. Springer Berlin Heidelberg, 2008.
- 405 [22] K. Li and H. Tian. Adaptive Differential Evolution with Evolution Memory for Multiobjective Optimization. *IEEE Access*, 7:866–876, 2019.
- [23] Y. J. Liu, Q. Sun, and X. L. Fan. A non-intrusive global/local algorithm with non-matching interface: Derivation and numerical validation. *Computer Methods in Applied Mechanics and Engineering*, 277(August):81–103, 2014.
- 410 [24] M. Locatelli. On the Multilevel Structure of Global Optimization Problems. *Computational Optimization and Applications*, 30(1):5–22, jan 2005.
- [25] L. D. Lorenzis. *Modeling in Engineering Using Innovative Numerical Methods for Solids and Fluids*, volume 599 of *CISM International Centre for Mechanical Sciences*. Springer International Publishing, Cham, 2020.

- 415 [26] Y. Q. Marinho, F. Fruett, and M. Giesbrecht. Application of differential evolution to multi-objective tuning of vibration spectrum analyzers based on microelectromechanical systems. *Engineering Applications of Artificial Intelligence*, 97:104071, 1 2021.
- [27] C. Negrello, P. Gosselet, and C. Rey. A new impedance accounting for short- and long-range effects in mixed substructured formulations of nonlinear problems. *International Journal for Numerical Methods in Engineering*, 114(7):675–693, 2018.
- 420 [28] N. Noii, F. Aldakheel, T. Wick, and P. Wriggers. An adaptive global–local approach for phase-field modeling of anisotropic brittle fracture. *Computer Methods in Applied Mechanics and Engineering*, 361:112744, 4 2020.
- [29] B. Olson, I. Hashmi, K. Molloy, and A. Shehu. Basin Hopping as a General and Versatile Optimization Framework for the Characterization of Biological Macromolecules. *Advances in Artificial Intelligence*, 2012:1–19, dec 2012.
- 425 [30] P. Oumaziz, P. Gosselet, P.-a. Boucard, and S. Guinard. A non-invasive implementation of a mixed domain decomposition method for frictional contact problems. *Computational Mechanics*, 60(5):797–812, 11 2017.
- [31] P. Oumaziz, P. Gosselet, K. Saavedra, and N. Tardieu. Analysis, improvement and limits of the multiscale Latin method. *Computer Methods in Applied Mechanics and Engineering*, 384:113955, oct 2021.
- 430 [32] J.-c. Passieux, J. Réthoré, A. Gravouil, and M.-C. Baietto. Local / global non-intrusive crack propagation simulation using a multigrid X-FEM solver. *Computational Mechanics*, 52(6):1381–1393, 2013.
- [33] F.-X. Roux. Domain decomposition methodology with robin interface matching conditions for solving strongly coupled problems. pages 311–320. Springer Berlin Heidelberg, 2008.
- 435 [34] K. Saavedra, O. Allix, P. Gosselet, J. Hinojosa, and A. Viard. An enhanced nonlinear multi-scale strategy for the simulation of buckling and delamination on 3D composite plates. *Computer Methods in Applied Mechanics and Engineering*, 317:952–969, 2017.
- [35] S. E. Schönborn, S. Goedecker, S. Roy, and A. R. Oganov. The performance of minima hopping and evolutionary algorithms for cluster structure prediction. *Journal of Chemical Physics*, 130(14):144108, apr 2009.
- 440 [36] P. Virtanen, R. Gommers, T. E. Oliphant, M. Haberland, T. Reddy, D. Cournapeau, E. Burovski, P. Peterson, W. Weckesser, J. Bright, S. J. van der Walt, M. Brett, J. Wilson, K. J. Millman, N. Mayorov, A. R. J. Nelson, E. Jones, R. Kern, E. Larson, C. J. Carey, I. Polat, Y. Feng, E. W. Moore, J. VanderPlas, D. Laxalde, J. Perktold, R. Cimrman, I. Henriksen, E. A. Quintero, C. R. Harris, A. M. Archibald, A. H. Ribeiro, F. Pedregosa, and P. van Mulbregt. SciPy 1.0: fundamental algorithms for scientific computing in Python. *Nature Methods*, 17(3):261–272, 3 2020.
- 445 [37] D. J. Wales and J. P. K. Doye. Global Optimization by Basin-Hopping and the Lowest Energy Structures of Lennard-Jones Clusters Containing up to 110 Atoms. *The Journal of Physical Chemistry A*, 101(28):5111–5116, 7 1997.
- [38] J. D. Whitcomb. Iterative global/local finite element analysis. *Computers and Structures*, 40(4):1027–1031, 1991.
- 450 [39] S. Yasear and K. R. Ku-Mahamud. Review of the multi-objective swarm intelligence optimization algorithms. *Journal of Information and Communication Technology*, 20(2):171–211, 2021.
- [40] C. Zhou, C. Ieritano, and W. S. Hopkins. Augmenting Basin-Hopping With Techniques From Unsupervised Machine Learning: Applications in Spectroscopy and Ion Mobility, aug 2019.